

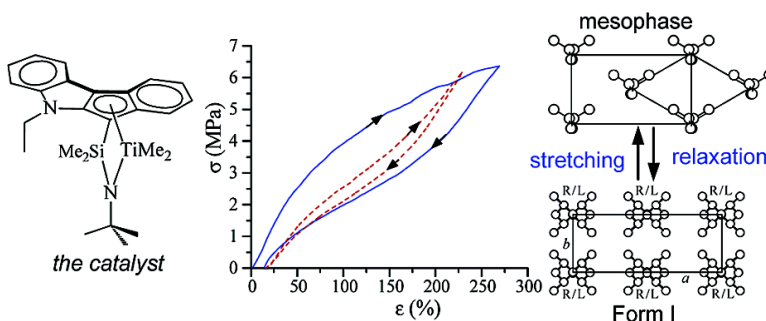
## Synthesis and Characterization of High-Molecular-Weight Syndiotactic Amorphous Polypropylene

Claudio De Rosa, Finizia Auriemma, Odda Ruiz de Ballesteros, Luigi Resconi, Anna Fait, Eleonora Ciaccia, and Isabella Camurati

*J. Am. Chem. Soc.*, **2003**, 125 (36), 10913-10920 • DOI: 10.1021/ja035911y • Publication Date (Web): 14 August 2003

Downloaded from <http://pubs.acs.org> on March 29, 2009

Thermoplastic elastomeric *syndiotactic amorphous* polypropylene.



### More About This Article

Additional resources and features associated with this article are available within the HTML version:

- Supporting Information
- Links to the 2 articles that cite this article, as of the time of this article download
- Access to high resolution figures
- Links to articles and content related to this article
- Copyright permission to reproduce figures and/or text from this article

[View the Full Text HTML](#)

## Synthesis and Characterization of High-Molecular-Weight Syndiotactic Amorphous Polypropylene

Claudio De Rosa,\* Finizia Auriemma, Odda Ruiz de Ballesteros, Luigi Resconi, Anna Fait, Eleonora Ciaccia, and Isabella Camurati

Contribution from the Dipartimento di Chimica, Università di Napoli "Federico II", Complesso Monte S. Angelo, Via Cintia, 80126 Napoli, Italy and Basell Polyolefins, Centro Ricerche G. Natta, P.le G. Donegani 12, I-44100 Ferrara, Italy

Received May 2, 2003; E-mail: derosa@chemistry.unina.it

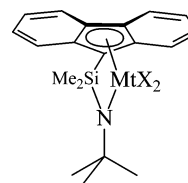
**Abstract:** Heterocycle-fused titanium indenyl silylamido dimethyl complexes produce very high molecular weight polypropylene having a prevalently syndiotactic microstructure with syndiotactic pentad contents *rrrr* up to 40–55% (*sam*-PP). The samples are basically amorphous and may slowly develop a low level of crystallinity (16–20%) at room temperature. A structural characterization has shown that *sam*-PP samples crystallize in disordered modifications of the helical form I of syndiotactic polypropylene (s-PP). The stretching of compression-molded films of *sam*-PP samples produce oriented crystalline fibers in the trans-planar mesomorphic form of s-PP. The low stereoregularity prevents the formation of the ordered trans-planar form III of s-PP, which instead is obtained in stretched fibers of the highly stereoregular and crystalline s-PP. The trans-planar mesomorphic form, obtained in stretched fibers, in turn transforms into the helical form I upon releasing the tension. The analysis of the mechanical properties has shown that *sam*-PP samples show good elastic behavior in a large range of deformation with remarkable strength, due to the presence of crystallinity. A comparison with the mechanical properties of less syndiotactic and fully amorphous samples is reported. These fully amorphous samples present lower strength and experience rapid viscous flow of the chains at high deformations and/or by application of stresses for long times. The higher strength in the semicrystalline *sam*-PP samples makes these materials interesting thermoplastic elastomers showing high toughness and ductility.

### Introduction

Titanium cyclopentadienylsilylamido complexes<sup>1,2</sup> are able to polymerize propylene to amorphous polypropylene (*am*-PP) with molecular weights and activities that depend on the substitution of the cyclopentadienyl (Cp) ring.<sup>3–5</sup> In several cases, very high molecular weights have been obtained.<sup>6,7</sup>

Some attempts have been made in order to introduce a stereoselecting ability by means of ligand substitution. While the use of asymmetric amides has not imparted enantioface differentiation in propene insertion, the use of bulky Cp ligands has been more successful. Okuda has prepared a zirconium fluorenyl *tert*-butylamido complex (Chart 1, Mt = Zr), "...in order to examine the detailed complexation behavior of this novel chelating ligand type—i.e. the linked Cp—amido ligands—also for potentially syndiospecific metallocene catalysts..."<sup>8</sup>

Chart 1. <sup>a</sup>



<sup>a</sup> Legend: Mt = Ti, Zr; X = Cl, Me.

The analogous Ti complex has been described by Shiono<sup>9</sup> and shown to polymerize propylene to moderately syndiotactic polypropylene, in accordance with Okuda's prediction. Busico has shown that stereodifferentiation arises from site control,<sup>10</sup> quite to be expected in a complex having the *C<sub>s</sub>* symmetry required for syndiospecificity.<sup>11</sup>

More recently, the AtoFina group has reported on a more syndioselective ligand design, based on the use of di-*tert*-butyl-substituted fluorenyl ligands (Chart 2).<sup>12,13</sup>

These Ti complexes, [Me<sub>2</sub>Si(2,7-*t*-Bu<sub>2</sub>Flu)(*t*-BuN)]TiCl<sub>2</sub><sup>12</sup> and, better, [Me<sub>2</sub>Si(3,6-*t*-Bu<sub>2</sub>Flu)(*t*-BuN)]TiCl<sub>2</sub>,<sup>13</sup> give high-

<sup>†</sup> Università di Napoli.

<sup>‡</sup> Centro Ricerche G. Natta.

- (1) Stevens, J. C.; Timmers, F. J.; Wilson, D. R.; Schmidt, G. F.; Nickias, P. N.; Rosen, R. K.; Knight, G. W.; Lais, S. Y. (Dow Chemical Company) Eur. Pat. Appl. 0 416 815, 1990.
- (2) Stevens, J. C. *Stud. Surf. Sci. Catal.* **1994**, *89*, 277.
- (3) McKnight, A. L.; Waymouth, R. M. *Chem. Rev.* **1998**, *98*, 2587.
- (4) Resconi, L. In *Metallocene Catalysts*; Kaminsky, W., Scheirs, J., Eds.; Wiley: New York, 1999; pp 467–484.
- (5) Resconi, L.; Camurati, I.; Grandini, C.; Rinaldi, M.; Mascellani, N.; Traverso, O. *J. Organomet. Chem.* **2002**, *664*, 5.
- (6) Canich, J. A. M. (Exxon) U.S. Patent 5 504 169, 1996.
- (7) Canich, J. A. M. (Exxon) U.S. Patent 5 026 798, 1991.

- (8) Okuda, J.; Schattenmann, F. J.; Wokadlo, S.; Massa, W. *Organometallics* **1995**, *14*, 789.
- (9) Hagihara, H.; Shiono, T.; Ikeda, T. *Macromolecules* **1997**, *30*, 4783.
- (10) Busico, V.; Cipullo, R. *Prog. Polym. Sci.* **2001**, *26*, 443.
- (11) Resconi, L.; Cavallo, L.; Fait, A.; Piemontesi, F. *Chem. Rev.* **2000**, *100*, 1253 and references therein.

Chart 2

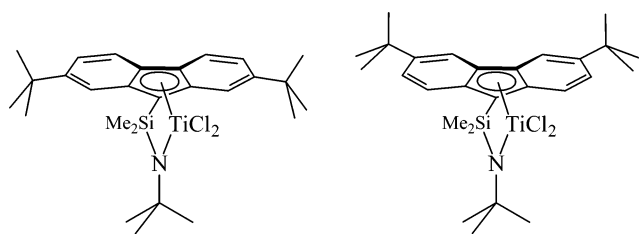
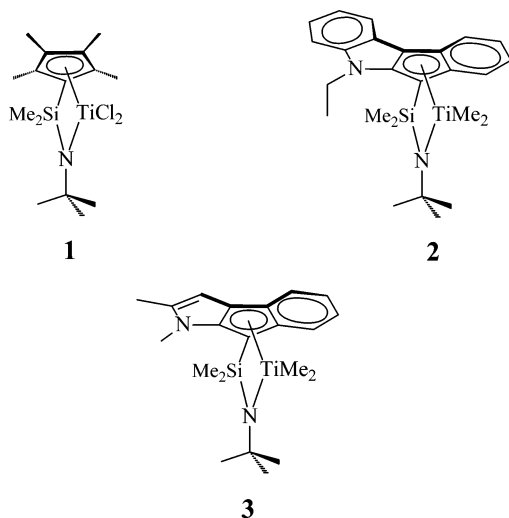


Chart 3



molecular-weight syndiotactic polypropylene with high activity. Although the polymers show only very limited crystallinity, *rrrr* pentad contents reach well above 70%.

We have recently described silyl-bridged indenyl *tert*-butylamido complexes of Ti in which the indenyl ligand has a heterocycle condensed onto the Cp moiety<sup>14,15</sup> (**2** and **3** in Chart 3). These complexes are highly active and produce *syndiotactic amorphous* polypropylenes (*sam*-PP) of very high molecular weights. Here we describe the preparation of *sam*-PP with controlled particle morphology from supported catalysts and its physical characterization. The mechanical properties of *sam*-PP samples are compared with those of less syndiotactic and fully amorphous samples (*am*-PP) prepared with Dow's Me<sub>2</sub>Si(Me<sub>4</sub>Cp)(*t*-BuN)TiCl<sub>2</sub>/MAO catalyst<sup>1</sup> (**1** in Chart 3).

## Experimental Section

**General Procedures.** The synthesis of complexes **2** and **3** has been carried out as described in refs 14 and 15.

Al(*i*-Bu)<sub>3</sub> (Witco) was used as a 1 M hexane (liquid propylene tests) or toluene solution, and MAO (methylalumoxane, Witco) was purchased as a 10 wt % solution in toluene and then used as received (liquid propylene tests) or dried under vacuum to remove most of the free

trimethylaluminum. Immediately before use, the glassy powder so obtained was redissolved in toluene to 1 M in Al (solution tests). Polymerization grade propylene was obtained from Basell Ferrara plants.

**Liquid Propylene Polymerizations with Unsupported Catalysts.** Homogeneous polymerizations were carried out as follows: 1 mmol of Al(*i*-Bu)<sub>3</sub> (as hexane solution) and the required amount of propylene were charged, at room temperature, in a 1 L jacketed stainless steel autoclave, equipped with magnetically driven stirrer and a 35 mL stainless steel vial, connected to a thermostat for temperature control, previously purified by washing with an Al(*i*-Bu)<sub>3</sub> solution in hexane and dried at 50 °C under a stream of propylene. The autoclave was then thermostated at 2 °C below the polymerization temperature, and the catalyst system, prepared by dissolving the Ti complex in the required amount of MAO/toluene solution and aging for 10 min at room temperature, was injected in the autoclave by means of nitrogen pressure through the stainless steel vial. Polymerizations were carried out at constant temperature and pressure for 1 h and then stopped by adding CO (5 bar); the residual monomer was vented, the reactor cooled, and the polymer dried at 60 °C under reduced pressure.

**Preparation of the Supported Catalysts. (a) Polyethylene Carrier.** The polyethylene used as the carrier was prepared by a Ziegler–Natta catalyst, polymerizing ethylene up to a conversion of 40 g<sub>PE</sub>/g<sub>cat</sub>. The prepolymer was treated with steam in order to deactivate the Ziegler–Natta catalyst, washed with hexane for 6 h using a Soxhlet apparatus, dried under a nitrogen flow at 110 °C, and sieved to obtain the desired diameter range (300–425 μm). The porosity measured by the mercury porosimeter technique is about 50% v/v. The surface area is 5.6 m<sup>2</sup>/g, and the mean pore diameter is 8923 Å.

**(b) Impregnation.** The apparatus used for the supportation is a glass cylindrical vessel, equipped with a vacuum pump, a dosing pump for the feeding of the catalytic solution on the carrier, and a stirrer to allow good mixing during the impregnation step.<sup>16</sup> The preparation of the supported catalysts is carried out under nitrogen flow at room temperature. A 5 g portion of the PE carrier described above is loaded into the vessel and mechanically stirred under nitrogen flow; a solution prepared by diluting 0.4 mL of a MAO solution (Albemarle, 300 g/L in toluene) with 2 mL of toluene is dosed in a single addition step onto the carrier to scavenge residual impurities, to reach the incipient wetness. The solvent is then evaporated under vacuum. The catalytic solution is prepared by dissolving 72 mg of **3** in 7.1 mL of the same MAO solution, with the aim of achieving an Al/Ti mole ratio of 200. This solution is stirred for 15 min and then is added to the carrier in three aliquots; after each addition, once the incipient wetness is reached, the solvent is evaporated under vacuum. The analysis of the obtained supported catalyst is as follows: Al, 11.65 wt % (4.23 mmol Al/g support); Ti, 0.13 wt % (0.0271 mmol Ti/g support); Al/Ti = 160.

**Liquid Propylene Polymerizations with PE-Supported Catalyst.** The 4.25 L stainless steel stirred reactor is purified by washing with 2 L of hexanes containing 5–6 mL of 10% TEA (1 M), stirring for 1 h at 70 °C, and discharging through the bottom valve under N<sub>2</sub> pressure. Then 2 L of propylene is charged, stirred for 1 h at 70 °C, and discharged through the bottom valve to the flare; at this point, the reactor temperature is lowered to 30 °C and the reactor pressure to 0.5 bar g. Then the scavenger (4 mL of 1 M TEA in hexane) is added under a propylene stream, and 1200 g of liquid propylene is loaded into the reactor at 30 °C (and hydrogen when requested) in order to have a liquid volume of 3 L at the polymerization temperature. The supported catalyst is then injected as a dry powder into the reactor by means of nitrogen overpressure through a stainless steel vial; then the vial is rinsed with 3–4 mL of hexane into the reactor, again with N<sub>2</sub> overpressure, and the temperature of the reactor is raised to the polymerization temperature in 10 min.

Polymerizations are carried out at constant temperature and pressure, and then the residual monomer is vented, the reactor cooled and purged

- (12) Razavi, A.; Bellia, V.; De Brauwer, Y.; Hortmann, K.; Lambrecht, M.; Miserque, O.; Peters, L.; Van Belle, S., Ed.; *Metalorganic Catalysts for Synthesis and Polymerization*; Kaminsky, W., Ed.; Springer-Verlag: Berlin, 1999. Razavi, A. Eur. Pat. Appl. 96111127, 1996. Razavi, A. (Atofina) PCT/EP97/036449, Int. Appl. WO 98/02469, 1998. Haveaux, B.; Coupin, T. (Atofina) PCT/EP99/00371, Int. Appl. WO 99/37711, 1999.
- (13) Razavi, A.; Thewalt, U. J. *Organomet. Chem.* **2001**, 621, 267. Razavi, A. (Atofina) PCT/EP00/08883, Int. Appl. WO 01/19877, 2001.
- (14) Grandini, C.; Camurati, I.; Guidotti, S.; Mascellari, N.; Resconi, L.; Nifant'ev, I. E.; Kashulin, I. A.; Ivchenko, P. V.; Mercandelli, P.; Sironi, A. Submitted for publication in *Organometallics*.
- (15) Resconi, L.; Guidotti, S.; Baruzzi, G.; Grandini, C.; Nifant'ev, I. E.; Kashulin, I. A.; Ivchenko, P. V. (Basell: Italy) PCT Int. Appl. WO 01/53360, 2001.

- (16) Covezzi, M.; Fait, A. (Basell: Italy) PCT Int. Appl. WO 01/44319 2001.

**Table 1.** Propylene Polymerization with Catalysts 1–3 (Nonsupported)<sup>a</sup>

run	cat.	amt of cat. (mg)	MAO/Ti molar ratio	$T_p$ (°C)	amt of H <sub>2</sub> (mL)	time (min)	productivity (kg <sub>ppf</sub> / (g <sub>cat</sub> h))	IV (dL/g)	$M_n$	$T_m$ (°C)
samPP1	<b>2</b> <sup>c</sup>	0.5	1000	70		60	106	5.96	1 308 600	59
samPP2 <sup>b</sup>	<b>3</b>	1.4	1000	60		37	530	3.65	672 700	50
amPP6	<b>1</b>	1	3000	50		60	35	5.56	1 190 800	
amPP7	<b>1</b>	2	1000	60	100	60	24	2.42	385 200	

<sup>a</sup> Polymerization conditions: 1 L reactor, propylene 300 g, Al(*i*-Bu)<sub>3</sub> 1 mmol. <sup>b</sup> 4.2 L reactor. <sup>c</sup> The polymerization was started at 30 °C and the temperature raised to  $T_p$  in 5–7 min.  $T_p$  = polymerization temperature; IV = intrinsic viscosity;  $T_m$  = melting temperatures measured after 1 week of crystallization at room temperature.

with nitrogen, and the amorphous product collected and dried as described above.

**Hydrogen Effect.** To evaluate the influence of hydrogen on the molecular weight of the obtained polymers, propylene polymerization is carried out according to the procedure reported above, introducing different amounts of hydrogen before adding propylene (0, 50, and 100 NmL). The catalyst has a relatively good hydrogen response. With the amounts of hydrogen used, the intrinsic viscosity covers the range from 3.3 dL/g to 5.5 dL/g.

**Polymer Analysis in Solution.** Polymer <sup>13</sup>C NMR analysis is carried out as described in ref 14. The intrinsic viscosity (IV) is measured in tetrahydronaphthalene (THN) at 135 °C. The weight-average molecular weights of *sam*-PP and *am*-PP samples are obtained from their intrinsic viscosity values and the Mark–Houwink–Sakurada parameters derived by Pearson and Fetters:<sup>17</sup>  $[\eta] = (1.85 \times 10^{-4})\bar{M}_w^{0.737}$ .

**Structural Characterization.** Amorphous specimens of the *sam*-PP samples have been obtained by compression molding at 80 °C of as-polymerized samples. Crystallization of the samples has been performed by keeping the compression-molded specimens at room temperature for several days. A complete crystallization has been achieved in 1 week for all the crystallizable samples.

Oriented fibers of the *sam*-PP samples have been obtained by stretching at room temperature compression-molded samples after achieving the complete crystallization. Compression-molded films have been kept at room temperature for at least 1 week before stretching.

X-ray diffraction patterns have been obtained with Ni-filtered Cu K $\alpha$  radiation. The powder profiles were obtained with an automatic Philips diffractometer, whereas the fiber diffraction patterns were recorded on a BAS-MS imaging plate (FUJIFILM) using a cylindrical camera and processed with a digital imaging reader (FUJIBAS 1800). The X-ray fiber diffraction patterns have been recorded for stretched fibers soon after the stretching while keeping the fiber under tension, as well as for relaxed fibers, that is, after keeping the fiber under tension for 2 h and then removing the tension, allowing the complete relaxation of the specimens.

The melting temperatures of the semicrystalline samples were obtained with a Perkin-Elmer DSC-7 differential scanning calorimeter, performing scans under a flowing N<sub>2</sub> atmosphere and heating rate of 10 °C/min.

**Mechanical Characterization.** The mechanical tests have been performed on films prepared by compression molding. Powders of *sam*-PP and *am*-PP samples have been heated at 80 °C between perfectly flat brass plates under a press at very low pressure, kept at 80 °C for 5 min, and slowly cooled to room temperature. Special care has been taken to obtain films with uniform thickness (0.3 mm) and minimal surface roughness, according to the recommendation of the standard ASTM D-2292-85. Films obtained by compression molding have been kept at room temperature for at least 1 week before the tests, allowing complete crystallization in the case of the crystallizable samples.

The mechanical tests have been performed at room temperature with a miniature mechanical tester apparatus (Minimat, by Rheometrics Scientific), following the standard test method for tensile properties of

thin plastic sheeting ASTM D882-83. The ratio between the drawing rate and the initial length has been fixed equal to 0.1 mm/(mm min) for the measurement of Young's modulus and 10 mm/(mm min) for the measurement of stress–strain curves and the determination of the other mechanical properties (stress and strain at break and tension set). The values of the tension set have been measured according to the standard test method ASTM D412-87. The specimens of initial length  $L_0$  have been stretched up to a length  $L_t$ , i.e., up to the elongation  $\epsilon = [(L_t - L_0)/L_0]100$ , and held at this elongation for 10 min; then the tension is removed, and the final length of the relaxed specimens  $L_r$  is measured after 10 min. The tension set is calculated by using the following formula:  $t_s(\epsilon) = [(L_r - L_0)/L_0]100$ . The reported values of the mechanical properties are averaged over at least five independent experiments.

## Results and Discussion

The polypropylene samples investigated were prepared with the MAO-activated complexes shown in Chart 3. The synthesis of complexes **2** and **3** and their performance in propylene polymerization under different conditions has been reported previously.<sup>14,15</sup>

**Polymerization in Liquid Monomer: Homogeneous Systems.** The polymerization results obtained with **2**/MAO and **3**/MAO are listed in Table 1, compared with Dow's Me<sub>2</sub>Si(Me<sub>4</sub>Cp)(*t*-BuN)TiCl<sub>2</sub>/MAO catalyst (**1**/MAO).<sup>1</sup>

The catalysts **2**/MAO and **3**/MAO show a high activity in propylene polymerization, producing soft, nonsticky, apparently elastic polypropylenes of very high molecular weights and a prevalently syndiotactic microstructure ( $[rrrr] = 50\text{--}55\%$ ) with no measurable regioerrors (2,1- or 3,1-insertions). As polymerized, their DSC traces show no melting transitions. We have dubbed these syndiotactic amorphous polypropylenes "*sam*-PP". Catalyst activity, PP molecular weights, and syndiotacticity are higher with **2** and **3** compared to **1**. These properties—most remarkably the high molecular weights—are maintained even at the relatively high polymerization temperature of 80 °C. In addition, syndiotacticity is not affected by the polymerization temperature.

The methyl region of <sup>13</sup>C NMR of a typical *sam*-PP sample prepared with **3**/MAO is presented in Figure 1, together with that of a sample prepared with **1**/MAO (*am*-PP).

**Polymerization with Supported 3/MAO Catalyst.** **3**/MAO was supported on a polyethylene carrier (see Experimental Section for details) by following a Basell established technology<sup>16</sup> and tested under the same conditions as for the nonsupported systems. Three samples were prepared at different hydrogen levels. The results are shown in Table 2. Even supported, **3**/MAO shows a remarkably high activity and gives a product with outstanding (given the nature of this material) spherical morphology (Figure 2). Hence, PE-supported **3**/MAO enables the production, in liquid propylene, of spherical, free-flowing,

(17) Pearson, D., Fetters, L.; Younghouse, L.; Mays, J. *Macromolecules* **1988**, *21*, 478.

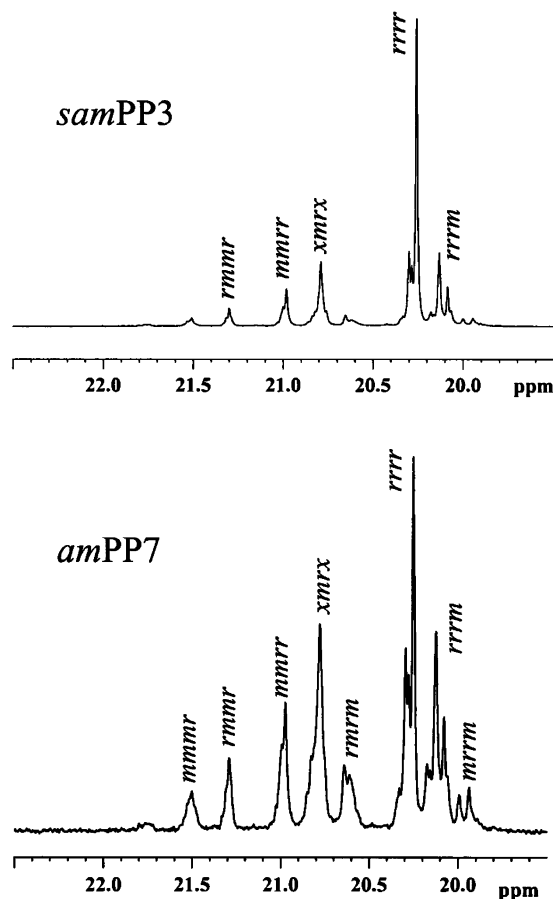


**Figure 1.** Methyl pentad region of  $^{13}\text{C}$  NMR spectra ( $\text{C}_2\text{D}_2\text{Cl}_4$ ,  $120^\circ\text{C}$ ) of the sample *samPP3* prepared with **3**/MAO in liquid monomer at  $80^\circ\text{C}$  (top) and of the sample *amPP7* prepared with **1**/MAO in liquid monomer at  $60^\circ\text{C}$  (bottom).

**Table 2.** Propylene Polymerization with PE-Supported **3**/MAO<sup>a</sup>

run	MAO/Ti molar ratio	H <sub>2</sub> (mL)	productivity (kg <sub>PP</sub> /(g <sub>cat</sub> h))	IV (dL/g)	<i>M<sub>w</sub></i>	<i>T<sub>m</sub></i> (°C)
<i>samPP3</i>	160	0	1.6	5.43	1 153 200	48
<i>samPP4</i>	160	50	2.1	4.47	885 700	48
<i>samPP5</i>	160	100	1.0	3.31	589 200	47

<sup>a</sup> Polymerization conditions: 4.2 L reactor, propylene 1500 g, polymerization temperature ( $T_p$ )  $80^\circ\text{C}$ , Al(*i*-Bu)<sub>3</sub> 1.5 mmol, polymerization started at  $30^\circ\text{C}$  and the temperature raised to  $T_p$  in 15 min, 1 h polymerization time. 300 mg catalyst, Al 11.7%, Ti 0.13%, Al/Ti = 160. IV = intrinsic viscosity;  $T_m$  = melting temperatures measured after 1 week of crystallization at room temperature.

soft, and resilient *sam*-PP, with no reactor fouling and with mileage up to 2 kg/(g<sub>cat</sub> h).

The results of the  $^{13}\text{C}$  NMR analysis of *sam*-PP samples prepared with catalysts **2** and **3** and *am*-PP samples prepared with catalyst **1** are reported in Table 3.

**Structural Characterization.** The structure and properties of syndiotactic polypropylene (*s*-PP) have been extensively studied.<sup>18–32</sup> A very complex polymorphic behavior has been

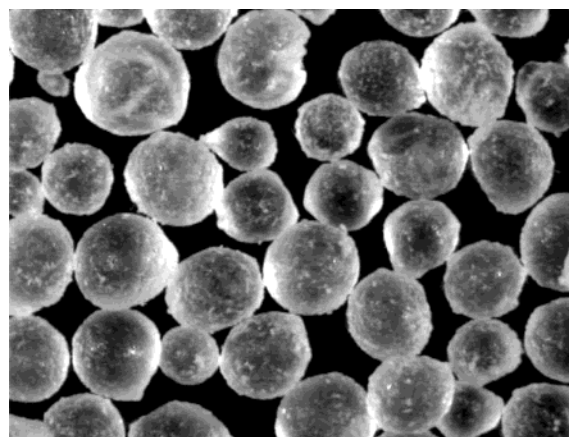


**Figure 2.** Optical microscope image of the sample *samPP5*, prepared with PE-supported **3**/MAO (particle size  $\sim 2$  mm).

described. Four different crystalline forms<sup>18–21,25–32</sup> and a mesomorphic form<sup>33,34</sup> have been found. The most stable form I and the metastable form II are characterized by chains in an  $s(2/1)2$  helical conformation, packed in orthorhombic unit cells.<sup>19,21,27–30</sup> The two metastable modifications, form III and form IV, present chains in trans-planar<sup>20,25</sup> and  $(\text{T}_6\text{G}_2\text{T}_2\text{G}_2)_n$ <sup>26,32</sup> helical conformations, respectively. A polymorphic transition between the trans-planar form III and the isochiral helical form II has been observed in oriented fibers.<sup>30</sup> The trans-planar form III can be obtained by stretching at room temperature highly stereoregular *s*-PP samples.<sup>25,27</sup> It transforms into the isochiral helical form II by releasing the tension.<sup>30,35</sup> This transition is reversible; the trans-planar form III and the helical form II transform each other by stretching and relaxing oriented fibers.<sup>30,35,36</sup>

It has been reported that the stereoregularity of *s*-PP samples strongly influences the polymorphic behavior.<sup>29–31,35</sup> Changes in the polymorphic behavior of *s*-PP in low stereoregular *sam*-PP samples is, therefore, expected.

As-prepared *sam*-PP samples, prepared with catalysts **2** and **3** (samples *samPP1*–*samPP5*), are generally amorphous. Moreover, they do not crystallize by cooling the melt to room temperature but slowly crystallize if the samples are kept at room temperature for several days. The X-ray powder diffraction profiles of compression-molded films of the *sam*-PP samples are reported in Figure 3.

The X-ray diffraction patterns of Figure 3 have been recorded after keeping the compression-molded films at room temperature for 1 week to allow the complete crystallization of the

- (18) Natta, G.; Corradini, P.; Ganis, P. *Makromol. Chem.* **1960**, *39*, 238.  
 (19) Corradini, P.; Natta, G.; Ganis, P.; Temussi, P. A. *J. Polym. Sci., Part C* **1967**, *16*, 2477.  
 (20) Natta, G.; Peraldo, M.; Allegra, G. *Makromol. Chem.* **1964**, *75*, 215.  
 (21) Lotz, B.; Lovinger, A. J.; Cais, R. E. *Macromolecules* **1988**, *21*, 2375.  
 (22) Lovinger, A. J.; Lotz, B.; Davis, D. D. *Polymer* **1990**, *31*, 2253.  
 (23) Lovinger, A. J.; Davis, D. D.; Lotz, B. *Macromolecules* **1991**, *24*, 552.  
 (24) Lovinger, A. J.; Lotz, B.; Davis, D. D.; Padden, F. J. *Macromolecules* **1993**, *26*, 3494.

- (25) Chatani, Y.; Maruyama, H.; Noguchi, K.; Asanuma, T.; Shiomura, T. *J. Polym. Sci., Part C* **1990**, *28*, 393.  
 (26) Chatani, Y.; Maruyama, H.; Asanuma, T.; Shiomura, T. *J. Polym. Sci., Polym. Phys.* **1991**, *29*, 1649.  
 (27) De Rosa, C.; Corradini, P. *Macromolecules* **1993**, *26*, 5711.  
 (28) De Rosa, C.; Auriemma, F.; Corradini, P. *Macromolecules* **1996**, *29*, 7452.  
 (29) De Rosa, C.; Auriemma, F.; Vinti, V. *Macromolecules* **1997**, *30*, 4137.  
 (30) De Rosa, C.; Auriemma, F.; Vinti, V. *Macromolecules* **1998**, *31*, 7430.  
 (31) De Rosa, C.; Auriemma, F.; Vinti, V.; Galimberti, M. *Macromolecules* **1998**, *31*, 6206.  
 (32) Auriemma, F.; De Rosa, C.; Ruiz de Ballesteros, O.; Vinti, V. *J. Polym. Sci., Polym. Phys.* **1998**, *36*, 395.  
 (33) Nakaoki, T.; Ohira, Y.; Hayashi, H.; Horii, F. *Macromolecules* **1998**, *31*, 2705.  
 (34) Vittoria, V.; Guadagno, L.; Comotti, A.; Simonutti, R.; Auriemma, F.; De Rosa, C. *Macromolecules* **2000**, *33*, 6200.  
 (35) Auriemma, F.; Ruiz de Ballesteros, O.; De Rosa, C. *Macromolecules* **2001**, *34*, 4485.  
 (36) De Rosa, C.; Gargiulo, M. C.; Auriemma, F.; Ruiz de Ballesteros, O.; Razavi, A. *Macromolecules* **2002**, *35*, 9083.

**Table 3.**  $^{13}\text{C}$  NMR Analysis of *sam*-PP and *am*-PP Samples<sup>a</sup>

sample	$T_p^b$ (°C)	<i>mmmm</i> (%)	<i>mmmr</i> (%)	<i>rmmr</i> (%)	<i>mmrr</i> (%)	<i>xmrx</i> (%)	<i>rmrm</i> (%)	<i>rrrr</i> (%)	<i>rrrm</i> (%)	<i>mrrm</i> (%)	<i>m</i> (%)	<i>r</i> (%)	$a^c$	$P_{bs}^d$	2,1 <sup>e</sup>
<i>sam</i> PP1	70	0.31	1.75	2.90	8.81	10.32	2.38	54.62	16.31	2.59	15.73	84.27	0.9351	0.0676	~0.2
<i>sam</i> PP2	60	0.00	1.36	2.91	7.05	13.69	2.83	51.60	17.52	3.04	16.06	83.94	0.9511	0.1005	~0.1
<i>sam</i> PP3	80	0.53	2.01	3.24	7.73	14.81	3.84	45.84	18.64	3.36	18.97	81.03	0.9410	0.1161	≤0.3
<i>sam</i> PP4	80	0.27	2.14	3.39	7.55	13.76	3.66	46.86	18.02	4.35	18.29	81.72	0.9378	0.1068	≤0.3
<i>sam</i> PP5	80	0.78	2.69	3.75	8.84	15.63	4.64	41.42	18.33	3.92	21.77	78.23	0.9264	0.1231	≤0.3
<i>am</i> PP6	50	0.76	3.53	5.24	9.96	19.53	8.60	26.52	19.57	6.29	28.57	71.43	0.9127	0.2109	1.13
<i>am</i> PP7	60	0.95	3.56	5.24	10.23	20.14	8.75	25.73	19.56	5.84	29.31	70.69	0.9155	0.2205	0.90

<sup>a</sup> Assignment of resonances as in ref 10. <sup>b</sup>  $T_p$  = polymerization temperature. <sup>c</sup> Probability of syndiotactic placement. <sup>d</sup> Probability of back-skip. <sup>e</sup> Concentration of 2,1-regioerrors.

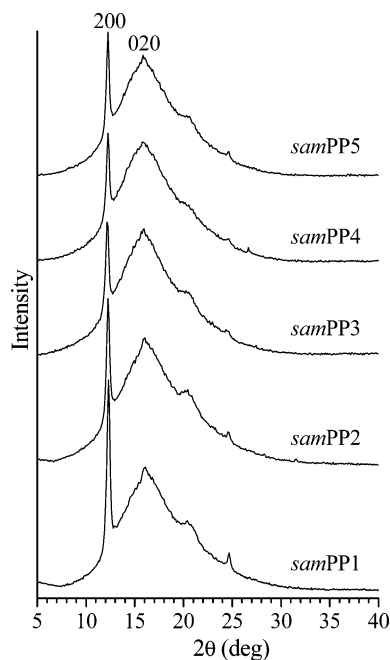


**Figure 3.** X-ray powder diffraction profiles of compression-molded films of *sam*-PP samples. The films obtained by compression molding have been kept at room temperature for 1 week to allow complete crystallization of the samples. The 200 and 020 reflections at  $2\theta = 12$  and  $16^\circ$ , respectively, of the helical form I of s-PP are indicated.

crystallizable samples. The samples *am*PP6 and *am*PP7, prepared with catalyst **1**, are amorphous and are not able to crystallize even for long aging times at room temperature. All the *sam*-PP samples crystallize in the helical form I of s-PP, as indicated by the presence in the X-ray diffraction profiles of Figure 3 of the 200 and 020 reflections at  $2\theta = 12$  and  $16^\circ$ , respectively. The diffraction patterns, however, indicate that disordered modifications of form I are obtained.<sup>29</sup> The absence of the 211 reflection at  $2\theta = 18.8^\circ$ , typical of the ordered form I,<sup>21</sup> indicates that disorder in the alternation of right- and left-handed helical chains along the axes of the unit cell is present.<sup>29</sup>

The degrees of crystallinity for all the samples are reported in Figure 4 as a function of the crystallization time at room temperature.

A maximum crystallinity of nearly 18–20% is achieved for the two more syndiotactic *sam*PP1 and *sam*PP2 samples ( $[rrrr] = 50$ –55%, Table 3), with melting temperatures of 59 and 50 °C, respectively. The crystallization is faster for the higher molecular weight sample. A lower crystallinity of nearly 16% is instead achieved for the less syndiotactic samples *sam*PP3, *sam*PP4, and *sam*PP5 ( $[rrrr] = 41$ –47%), regardless of the molecular weight, with melting temperatures of 47–48 °C.

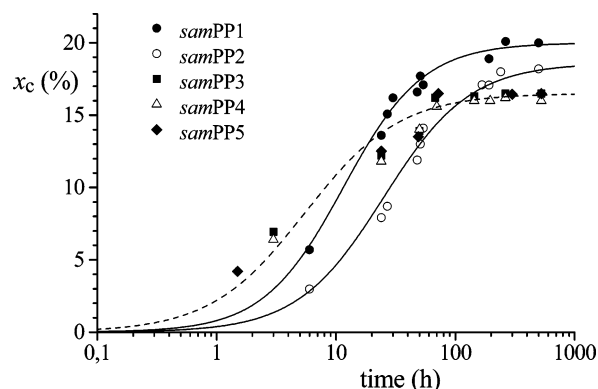


**Figure 4.** Degree of crystallinity of the *sam*-PP samples, evaluated from the X-ray powder diffraction profiles, as a function of the crystallization time at room temperature: (●) sample *sam*PP1; (○) sample *sam*PP2; (■) sample *sam*PP3; (△) sample *sam*PP4; (◆) sample *sam*PP5.

Oriented fibers of *sam*-PP samples have been obtained by stretching compression-molded films, after the complete crystallization in form I. The X-ray fiber diffraction pattern and the corresponding intensity profile read along the equatorial line (after subtraction of the amorphous halo) of fiber specimens of the sample *sam*PP1, obtained by stretching at 500% elongation and keeping the fiber under tension, are reported in parts A and A' of Figure 5, respectively. Similar patterns have been obtained for the other crystalline *sam*-PP samples.

It is apparent that fibers in the trans-planar disordered mesomorphic form are obtained, as indicated by the presence of a broad equatorial reflection in the range  $2\theta = 15$ – $18^\circ$ <sup>33,34</sup> and weak reflections on the first layer line corresponding to the periodicity of the trans-planar conformation (5.1 Å) in the pattern of Figure 5A,A'. The helical form I, present in the unstretched film, transforms into the trans-planar mesomorphic form by stretching at high deformations.

These data indicate that for these low syndiotactic *sam*-PP samples the ordered trans-planar form III does not form by stretching, as instead occurs for highly syndiotactic samples.<sup>25,27,30</sup> This confirms the data reported in the literature,<sup>27,30,35</sup> which indicate that the pure trans-planar form III can be obtained only for highly stereoregular s-PP samples, with syndiotactic pentad *rrrr* content higher than 90%. In the case of the *sam*-PP samples the very low stereoregularity does not prevent the formation of the trans-planar conformation, probably because the low crystallinity and the high molecular weight allow stretching at very high deformation, forming extended chains. However, the high concentration of defects prevents the packing of the trans-planar chains in the ordered lattice of form III, and only the disordered mesomorphic form is obtained (Figure 5).

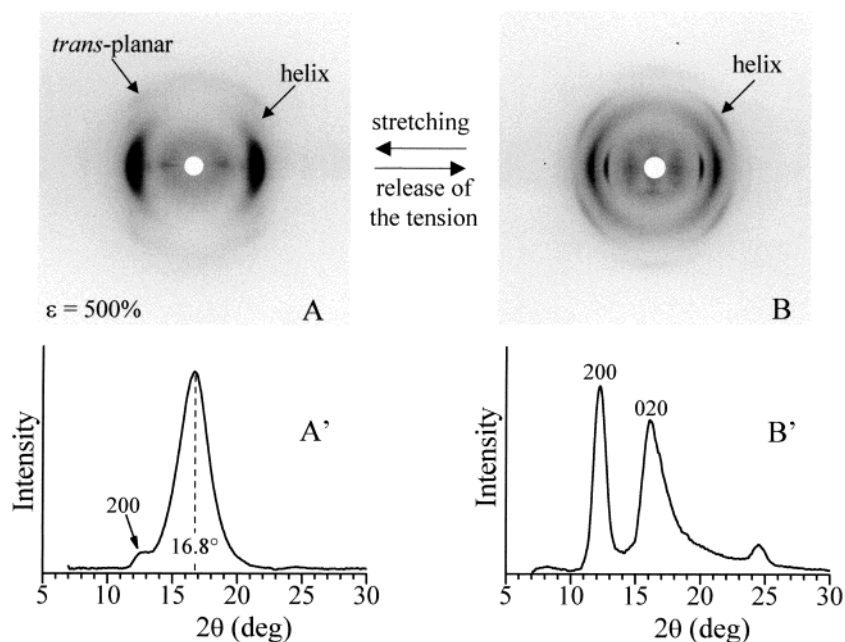


**Figure 5.** X-ray fiber diffraction patterns, after subtraction of the amorphous halo (A, B), and corresponding profiles read along the equatorial lines (A', B') of fibers of the sample *samPP1* obtained by stretching compression-molded films at 500% elongation, on keeping the fiber under tension (A, A') and after removing the tension (B, B'). The 200 and 020 reflections at  $2\theta = 12$  and  $16^\circ$ , respectively, typical of the helical form I of s-PP, and the broad reflection of the mesomorphic form at  $2\theta = 16.8^\circ$  are indicated. The fiber in A is in the trans-planar mesomorphic form, whereas the fiber in B is in the helical form I.

Similar behavior has been observed for the other semicrystalline *sam*-PP samples. The lowest syndiotactic samples *amPP6* and *amPP7* are amorphous and do not crystallize by stretching.

The X-ray diffraction pattern, and the corresponding equatorial profile (after subtraction of the amorphous halo), of the fiber of the sample *samPP1* stretched at 500% elongation (Figure 5A,A'), after releasing the tension, are reported in parts B and B' of Figure 5, respectively. It is apparent that, upon the release of the tension, the trans-planar mesomorphic form (Figure 5A) transforms into the helical form I, as indicated by the presence of the strong 200 and 020 reflections at  $2\theta = 12$  and  $16^\circ$ , typical of the helical form I, in the pattern of Figure 5B,B'. Similar behavior has been observed for the other crystalline *sam*-PP samples.

We recall that for highly syndiotactic polypropylene prepared with the classic metallocene catalyst of  $C_s$  symmetry (the prototypical syndiospecific metallocene of  $C_s$  symmetry is Ewen's  $\text{Me}_2\text{C}(\text{Cp})(\text{Flu})\text{ZrCl}_2$ ),<sup>37</sup> the stretching of films in the stable helical form I produces the formation of fibers in the trans-planar form III,<sup>25,27</sup> which transforms into the isochiral helical form II of s-PP after removing the tension.<sup>30,35</sup> The transition between the *trans*-planar form III and the helical form II is a reversible crystal–crystal transformation, as demonstrated by time-resolved diffraction experiments with synchrotron radiation.<sup>38</sup> The data of Figure 5 indicate that, for the low stereoregular *sam*-PP samples, the isochiral helical form II is never obtained, neither by stretching nor upon releasing the tension. This experimental observation confirms the hypothesis recently reported in the literature that the formation of the isochiral helical form II is strictly related to that of the trans-

planar form III of s-PP.<sup>35,36,38,39</sup> The isochiral helical form II can be obtained only from stretched fibers initially in the trans-planar form III through a spontaneous crystal–crystal transformation when the tension is removed.<sup>30,38,40</sup> When the trans-planar form III is absent, the most stable antichiral form I of s-PP forms in the fiber samples under any conditions.<sup>36,39</sup>

**Mechanical Properties.** The physical properties of highly stereoregular s-PP strongly depend on the polymorphic behavior. For instance, oriented fibers of s-PP show elastic behavior,<sup>35,36,41,42</sup> which is related to the structural organization. Unoriented compression-molded samples of s-PP behave like a typical highly crystalline material, showing a plastic deformation upon stretching at room temperature.<sup>35,36,42</sup> Only a partial recovery of the macroscopic dimensions of the sample is observed upon the release of the tension. Oriented fibers of s-PP show instead very good elastic behavior upon successive stretching and relaxation. The elastic recovery is associated with a reversible polymorphic transition between the trans-planar and helical forms. The helical form transforms by stretching into the trans-planar form, which transforms again into the helical form by releasing the tension, and a nearly total recovery of the initial dimensions of the fiber samples is observed.<sup>35,36</sup>

A study of the mechanical properties of high-molecular-weight syndiotactic polypropylene prepared by the Atofina group with the catalysts of Chart 2 has shown that this material presents good elastic behavior with values of the tensile strength and tensile modulus which decrease with decreasing stereoregular-

(37) Ewen, J. A.; Elder, M. J.; Jones, R. L.; Curtis, S.; Cheng, H. N. Catalytic Olefin Polymerization. In *Studies in Surface Science and Catalysis*; Keii, T., Soga, K., Eds.; Elsevier: New York, 1990; Vol. 56, p 439.

(38) Auriemma, F.; De Rosa, C. *J. Am. Chem. Soc.* In press.

(39) De Rosa, C.; Auriemma, F.; Orlando, I.; Talarico, G.; Caporaso, L. *Macromolecules* **2001**, *34*, 1663.

(40) Lotz, B.; Mathieu, C.; Thierry, A.; Lovinger, A. J.; De Rosa, C.; Ruiz de Ballesteros, O.; Auriemma, F. *Macromolecules* **1998**, *31*, 9253.

(41) Loos, J.; Schimanki, T. *Polym. Eng., Sci.* **2000**, *40*, 567.

(42) D'Aniello, C.; Guadagno, L.; Naddeo, C.; Vittoria, V. *Macromol. Chem. Rapid Commun.* **2001**, *22*, 104. Guadagno, L.; D'Aniello, C.; Naddeo, C.; Vittoria, V. *Macromolecules* **2001**, *34*, 2512. Guadagno, L.; D'Aniello, C.; Naddeo, C.; Vittoria, V.; Meille, S. V. *Macromolecules* **2002**, *35*, 3921.

**Table 4.** Elastic Modulus ( $E$ ), Stress ( $\sigma_b$ ) and Strain ( $\epsilon_b$ ) at Break, Stress ( $\sigma_y$ ) and Strain ( $\epsilon_y$ ) at the Yield Point, Tension Set at Break ( $t_b$ ), Tension Set at 400% Strain ( $t_s(400)$ ), and Crystallinity  $x_c$  of Unoriented Compression-Molded Films of *sam*-PP and *am*-PP Samples<sup>a</sup>

sample	[ <i>r</i> <i>r</i> <i>r</i> <i>r</i> ] (%)	$M_w$	$E$ (MPa)	$\sigma_b$ (MPa)	$\epsilon_b$ (%)	$\sigma_y$ (MPa)	$\epsilon_y$ (%)	$t_b$ (%)	$t_s(400)^b$ (%)	$x_c$ (%)
s-PP	93	213 000	256 ± 20	15 ± 1	400 ± 20	12 ± 1	10 ± 3	300 ± 10	300 ± 10	40
<i>sam</i> PP1	54.6	1 308 600	19 ± 4	7 ± 1	650 ± 60	3 ± 1	70 ± 5	59 ± 8	36 ± 1	20
<i>sam</i> PP2	51.6	672 700	14 ± 2	6 ± 1	531 ± 67	3 ± 1	110 ± 10	48 ± 2	31 ± 4	18
<i>sam</i> PP3	45.8	1 153 200	4 ± 1	4 ± 1	630 ± 80	2.4 ± 0.4	90 ± 10	12 ± 2	25 ± 1	16
<i>sam</i> PP4	46.9	885 700	1.2 ± 0.1	3 ± 1	580 ± 70	1.4 ± 0.2	82 ± 7	13 ± 3	25 ± 1	16
<i>sam</i> PP5	41.4	589 200	4 ± 1	3.0 ± 0.5	430 ± 60	2.2 ± 0.4	90 ± 6	17 ± 6		16
<i>am</i> PP6	26.5	1 190 800	0.5 ± 0.1	1.4 ± 0.1	880 ± 150	1.0 ± 0.1	130 ± 10	21 ± 8	8 ± 2	
<i>am</i> PP7	25.7	385 200	0.4 ± 0.1			0.5 ± 0.1	110 ± 10		11 ± 2	

<sup>a</sup> The fully syndiotactic pentad contents [*r**r**r**r*] and the molecular weights ( $M_w$ ) of the samples are also indicated. The data are compared with the mechanical properties of compression-molded films of the highly stereoregular and crystalline s-PP prepared with  $C_s$  catalyst.<sup>35</sup> <sup>b</sup> Values of the tension set ( $t_s(400)$ ) have been evaluated from samples of initial length  $L_0$ , stretched up to 400% elongation (final lengths  $L_f = 5L_0$ ), kept in tension for 10 min at room temperature and then relaxed by releasing the tension:  $t_s(\epsilon) = [(L_r - L_0)/L_0]100$ , with  $L_r$  being the final length after releasing the tension.

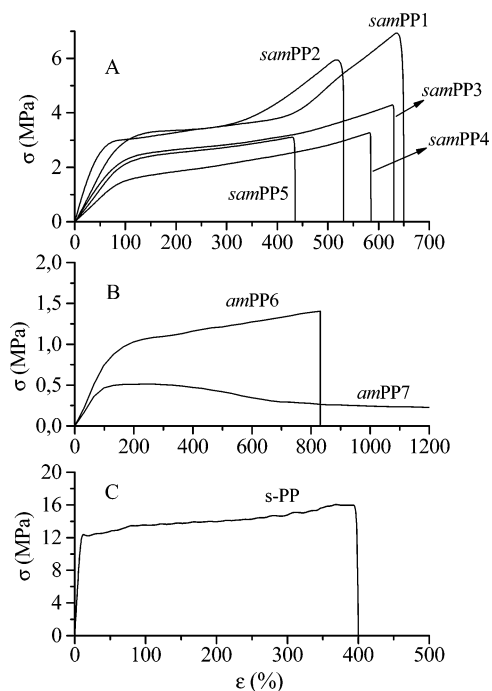


**Figure 6.** Stress–strain curves of unoriented compression-molded films of semicrystalline *sam*PP1–*sam*PP5 samples (A) and amorphous *am*PP6 and *am*PP7 samples (B). The stress–strain curve of a compression-molded film of highly stereoregular and crystalline s-PP prepared with  $C_s$ -symmetric catalyst, taken from ref 35, is also reported for comparison (C).

ity.<sup>12</sup> The increased softness is partly due to the increased length of atactic sequences in the prevailing syndiotactic chains.<sup>12</sup> In this section preliminary results of the analysis of the mechanical properties and the elastic behavior of the poorly crystalline *sam*-PP samples are reported and compared with the mechanical properties of highly stereoregular s-PP and of amorphous *am*-PP samples prepared with the catalyst 1/MAO.

The stress–strain curves of unoriented compression-molded films of semicrystalline *sam*-PP samples of Figure 3 (samples *sam*PP1–*sam*PP5) stretched at room temperature are reported in Figure 6A. The stress–strain curves of the lowest stereoregular amorphous samples *am*PP6 and *am*PP7 are reported in Figure 6B. These data are compared with the stress–strain curve of a compression-molded film of a highly stereoregular and crystalline s-PP sample prepared with the classic metallocene catalyst of  $C_s$  symmetry,<sup>37</sup> having a fully syndiotactic pentad content [*r**r**r**r*] of 93%, taken from ref 35 (Figure 6C).

The mechanical properties (Young’s modulus, stress and strain at break, stress and strain at yield, and tension set) of

*sam*-PP and *am*-PP samples are reported in Table 4 and compared with the data for the highly stereoregular s-PP. The values of the crystallinity of the starting compression-molded films are also reported in Table 4. It is apparent from Figure 6 and Table 4 that, because of the lower crystallinity, the “syndiotactic-amorphous” *sam*-PP samples show values of the mechanical properties (stress at any strain, tensile strength, and Young’s modulus) much lower than those of the highly stereoregular s-PP. All the *sam*-PP samples show strains at break higher than that observed for s-PP, indicating higher ductility in accord with the lower crystallinity. For the *sam*-PP samples a slight increase of the strain at break with decreasing crystallinity and increasing molecular weight is observed. Moreover, a higher tensile strength  $\sigma_b$  is observed for the more crystalline samples *sam*PP1 and *sam*PP2. The amorphous samples *am*PP6 and *am*PP7 show values of the strength much lower than those of the semicrystalline samples. In the case of sample *am*PP7, having the lowest molecular weight, high deformation without breaking and viscous flow for deformations higher than 500% are observed.

All the *sam*-PP samples show stress–strain curves typical of elastomers, with a small yielding. The values of the tension set,  $t_s(\epsilon) = [(L_r - L_0)/L_0]100$ , measured at room temperature for unoriented films stretched up to the break or up to deformation  $\epsilon = 400\%$  are also reported in Table 4. These values have been obtained by stretching unoriented films of initial length  $L_0$  up to the break, as in Figure 6, or up to the final length  $L_f = 5L_0$ , keeping the specimens in tension for 10 min, and then removing the tension and measuring the final length  $L_r$  of the relaxed sample after 10 min. The values of tension set at break and at 400% strain for unoriented films of highly crystalline s-PP are also reported in Table 4 for comparison.<sup>35</sup> The low values of tension set in Table 4 indicate that all the *sam*-PP samples experience a recovery of the initial dimension either after breaking or after removing the tension from a given deformation.

While unoriented films, not previously stretched, of highly stereoregular and crystalline s-PP samples show poor elastic properties after the first stretching,<sup>35,36,42</sup> “syndiotactic-amorphous” *sam*-PP samples show instead good elastic properties even after the first stretching of unoriented films (Table 4).

The amorphous sample *am*PP7, having the lowest molecular weight, experience a rapid viscous flow of the chains at deformations higher than 500% (Figure 6B) and/or by application of a constant stress. Therefore, for the amorphous *am*-PP samples prepared with the Dow’s catalyst 1/MAO, only when



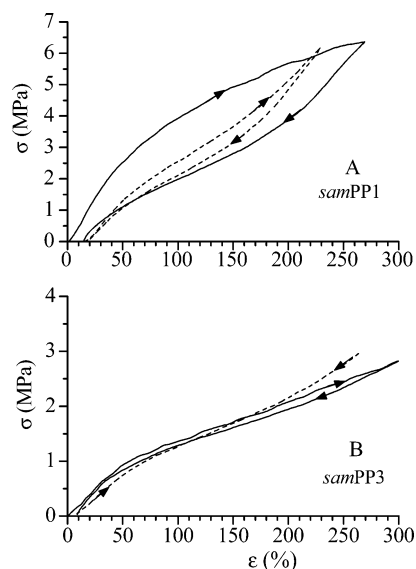


**Figure 7.** Stress–strain hysteresis cycles recorded at room temperature, composed of stretching and relaxation (at controlled rate) steps according to the direction of the arrows, for stress-relaxed fibers of the samples *samPP1* (A) and *samPP3* (B). The stress-relaxed fibers are prepared by stretching compression-molded films up to 400% elongation (final length  $L_f = 5L_0$ ) and then removing the tension. In the hysteresis cycles the stretching steps are performed, stretching the fibers up to the final length  $L_f = 5L_0$ . The first hysteresis cycle (continuous lines) and curves averaged for at least four cycles after to the first one (dashed lines) are reported.

the molecular weight is very high (sample *amPP6*) is the viscous flow prevented, giving interesting elastic properties but, however, very low strength. The presence of crystallinity in the samples *samPP1*–*samPP5*, prepared with **2**/MAO and **3**/MAO, increases the values of the modulus and the stress at any strain, making these materials interesting thermoplastic elastomers with higher strength.

To quantify the elastic properties of the fibers of *sam*-PP samples, hysteresis cycles have been performed at room temperature on the oriented stress-relaxed fibers. The hysteresis cycles, composed of the stress–strain curves measured during the stretching, immediately followed by the curves measured during the relaxation at controlled rate for the samples *samPP1* and *samPP3* are reported in Figure 7.

In these cycles, stress-relaxed oriented fibers of the new initial length  $L_r$  are stretched up to the final length  $L_f = 5L_0$ , with  $L_0$  being the initial length of the unoriented film. For each fiber, four successive cycles have been recorded; each cycle is performed after 10 min the end of the previous cycle. Successive hysteresis cycles, measured after the first one, are all nearly coincident, indicating a tension set close to zero.

These data indicate that both unoriented films and oriented fibers of the low-stereoregular, nearly amorphous *sam*-PP samples present good elastic properties in a large range of deformation.

## Conclusions

High-molecular-weight “*syndiotactic amorphous*” polypropylene (*sam*-PP) has been obtained with the heterocycle-fused

titanium indenyl silylamido dimethyl complexes **2** and **3**, activated by MAO, in liquid propylene, in the temperature range 60–80 °C. Their properties have been compared to those of *am*-PP samples obtained with Dow’s catalyst **1**.

As-prepared *sam*-PP and *am*-PP samples are generally amorphous. However, the slightly more stereoregular samples, having a syndiotactic pentad content *rrrr* of 40–55%, prepared with catalysts **2** and **3**, are able to crystallize. They do not crystallize by cooling the melt to room temperature but slowly crystallize at room temperature in several days in disordered modifications of form I of s-PP. A low degree of crystallinity, in the range 16–20%, is achieved.

The helical form I transforms into the trans-planar disordered mesomorphic form by stretching at high deformations. For these low syndiotactic *sam*-PP samples the ordered trans-planar form III does not form by stretching, as instead occurs for highly syndiotactic samples. This confirms the data reported in the literature<sup>27,30,35</sup> that the pure trans-planar form III can be obtained only for highly stereoregular s-PP sample. The trans-planar mesomorphic form transforms into the helical form I upon releasing the tension.

The analysis of the mechanical properties of the “*syndiotactic-amorphous*” *sam*-PP samples, prepared with catalysts **2** and **3**/MAO, has shown that these materials present a typical behavior of thermoplastic elastomers, where the small crystalline domains act as physical knots of the elastomeric lattice. All the *sam*-PP samples show good elastic behavior and strains at break higher than that observed for the highly crystalline s-PP, indicating higher ductility according to the lower crystallinity.

The comparison with the amorphous *am*-PP samples, prepared with the Dow’s catalyst **1**/MAO, show that the amorphous samples present lower strength and experience rapid viscous flow of the chains at high deformations and/or by application of stresses for long time. For these amorphous materials, only when the molecular weight is very high (sample *amPP6*) is the viscous flow prevented, giving interesting elastic properties but, however, very low strength. The presence of crystallinity in the samples *samPP1*–*samPP5*, prepared with **2**/MAO and **3**/MAO, increases the values of the modulus and the stress at any strain, making these materials interesting thermoplastic elastomers with higher strength.

For the semicrystalline *sam*-PP samples the elastic behavior is associated with a reversible polymorphic transition between the *trans*-planar mesomorphic form and the helical form I, which occurs during successive stretching and relaxing of fiber specimens. Therefore, since the small crystalline domains are characterized by a disordered modification (disordered form I), which transforms into the disordered mesomorphic form, they can be more easily plastically deformed.

**Acknowledgment.** Financial support from Basell and from the “Ministero dell’Istruzione, dell’Università e della Ricerca” (PRIN 2002 and Cluster C26 projects) are gratefully acknowledged.

JA035911Y